Pre-strain correction of forming limit curves

ARETZ Holger

Speira GmbH, Research & Development, Georg-von-Boeselager-Str. 21, 53117 Bonn, Germany

holger.aretz@speira.com

Abstract. Inherent features of the Nakajima test to determine forming limit curves (FLC) are inevitable bending strains and pre-strains originating from evolving punch contact in the early stage. Both effects are very annoying and bias the resulting FLC considerably, so that a direct comparison of materials with different gauges is impossible. In the present work, a simple computational procedure is developed to remove both effects from FLC data. Application examples demonstrate its capabilities.

Introduction

The forming limit curve (FLC) represents the transition from safe forming to failure and is thus an indispensable tool in sheet metal forming to ensure defect-free products. The most frequently used methodology in laboratory FLC-determination is the *Nakajima* approach. It involves stretch-forming of circular sheet samples possessing different symmetric cut-outs over a hemispherical punch to failure, so that a broad range of different strain modes can be realized, thereby providing a discrete picture of the FLC. In the present work, the standard FLC representation in terms of minor and major in-plane *true* strains at failure (denoted as ε_2 and ε_1, respectively, with the notational convention $\varepsilon_1 \geq \varepsilon_2$) will be considered, i.e. FLC $= f(\varepsilon_1, \varepsilon_2)$. Furthermore, the material of which the samples are made is approximated as *rigid-plastic*, i.e. elastic strains are neglected.

Despite its popularity the Nakajima method introduces two undesired effects: equibiaxial pre-strains caused by the evolving punch contact in the early stage of the test (see e.g. Noder & Butcher [9]), and strains associated with bending of the samples (see e.g. Affronti & Merklein [1]). Both effects bias the resulting FLC data in different ways:

1. Due to the presence of pre-strains, the realized strain-paths are essentially bi-linear (with the only exception of the equibiaxial strain mode, which is "immune" to equibiaxial pre-straining), thus violating an important prerequisite of FLC determination, viz. linearity of the imposed strain-paths. As a consequence, the FLC's minimum point, commonly called "FLC_{min}", is displaced to the *lower right* in strain space, i.e. FLC_{min} does not coincide with plane-strain deformation (as it should be the case) and its major strain value is usually lowered (see e.g. Müschenborn & Sonne [8]), provided that the bending strains do not dominate.

2. Bending strains act in the opposite direction and *lift* the major strain values. This is because strains measured on the convex side of a bent sample are always larger than, say, in the sample's midplane. This is a pure geometric effect and thus strongly dependent of the sample's thickness. Accordingly, if a (maybe material dependent) sample thickness is exceeded, the lowering effect of the pre-strains on the major strain of FLC_{min} can be overcompensated by the bending strains, in which case the FLC_{min}-point may be only slightly displaced in positive minor strain direction, but without altering or even elevating its major strain value compared to linear strain paths.

While the effect of bending strains does solely depend on the material's gauge, the pre-strain effect seems to be material dependent, at least according to the author's experience. Therefore, it is not

possible to compare materials with different gauges, which is very annoying in practice. This problem is addressed in the present work, and as a solution a simple computational method to remove both the pre-strains and the bending strains from the FLC data is proposed.

For notational convenience, throughout this paper the following 2×1 column matrices

$$\mathbf{FLC} := (\mathrm{FLC}_1, \mathrm{FLC}_2)^T, \ \mathbf{FLC}^* := (\mathrm{FLC}_1^*, \mathrm{FLC}_2^*)^T \ \text{and} \ \boldsymbol{\varepsilon}^* := (\varepsilon_1^*, \varepsilon_2^*)^T \tag{1}$$

will be used to store a strain tuple pertaining to a single point of the FLC, associated with zero and non-zero pre-strains $\boldsymbol{\varepsilon}^*$, respectively.

Forward Retro Analysis
The present work started with the development of a straightforward approach to reproduce given experimental or predicted FLCs using an elastic-plastic constitutive model: a given linear strain-path is incrementally followed until the target FLC is reached. Here, the key point is the formulation of a suitable termination criterion (cf. Eq. 3 below), which can handle pre-strains properly. This approach enables the acquisition of experimentally inaccessible data, such as stresses and work-conjugate equivalent plastic strains corresponding to the utilized constitutive model. This approach is called *forward retro analysis*, because a given FLC is *retrospectively* analyzed. Using concise notation, the forward retro analysis is written as

$$\mathbf{FLC}^* = \mathrm{retro}(\mathbf{FLC}, \boldsymbol{\varepsilon}^*) \tag{2}$$

In all cases, the following equation is to be solved (in an incremental approach this serves as a termination criterion to stop the accumulation of strain increments):

$$\|\boldsymbol{\varepsilon}^*\| + \|\mathbf{FLC}^* - \boldsymbol{\varepsilon}^*\| = \|\mathbf{FLC}\| \tag{3}$$

As a length measure, we define the following strain norm, which is a homogeneous function of degree one in terms of the strain components ε_1 and ε_2:

$$\eta(\varepsilon_1, \varepsilon_2) := \|\boldsymbol{\varepsilon}\| = \sqrt{\frac{2}{3} \cdot [\varepsilon_1^2 + \varepsilon_2^2 + \varepsilon_3^2]}, \quad \varepsilon_3 = -(\varepsilon_1 + \varepsilon_2) \tag{4}$$

Despite the fact that Eq. 4 is identical to the von Mises equivalent plastic strain definition, no isotropic material behavior is implied here, and Eq. 4 should be considered as a material independent and pure kinematic quantity.

To proceed, the strain difference

$$\Delta \mathbf{FLC}^* = (\Delta \mathrm{FLC}_1^*, \Delta \mathrm{FLC}_2^*)^T := \mathbf{FLC}^* - \boldsymbol{\varepsilon}^* \tag{5}$$

and the following strain ratio

$$\beta := \frac{\mathrm{FLC}_2}{\mathrm{FLC}_1} = \frac{\Delta \mathrm{FLC}_2^*}{\Delta \mathrm{FLC}_1^*} \tag{6}$$

are defined. In Eq. 6 two equivalent definitions of β are provided, and the one to be used depends on which input data are *known*, as will be become clear from the derivations that follow.

Using the strain norm Eq. 4, we may write:

$$\|\Delta \mathbf{FLC}^*\| = \Delta \mathrm{FLC}_1^* \cdot \eta(1, \beta) \quad \text{with} \quad \beta = \frac{\mathrm{FLC}_2}{\mathrm{FLC}_1} \tag{7}$$

Inserting Eq. 7 in Eq. 3 yields the strain differences

$$\Delta \text{FLC}_1^* = \frac{\|\mathbf{FLC}\| - \|\boldsymbol{\varepsilon}^*\|}{\eta(1,\beta)}, \ \ \Delta \text{FLC}_2^* = \beta \cdot \Delta \text{FLC}_1^* \tag{8}$$

Finally, inserting Eq. 8 into Eq. 5 gives the desired strain solutions

$$\text{FLC}_i^* = \varepsilon_i^* + \Delta \text{FLC}_i^*, \ \ i = 1,2 \tag{9}$$

Inverse Retro Analysis
As shown before, the forward retro analysis can be used to reproduce $\mathbf{FLC}^*$ using $\mathbf{FLC}$ and $\boldsymbol{\varepsilon}^*$ as input data, i.e. $\mathbf{FLC}^* = \text{retro}(\mathbf{FLC}, \boldsymbol{\varepsilon}^*)$. While this sounds not very useful at first glance, the true value of this procedure is revealed by *inverting* the process, called *inverse retro analysis*:

$$\mathbf{FLC} = \text{retro}^{-1}(\mathbf{FLC}^*, \boldsymbol{\varepsilon}^*) \tag{10}$$

Using the strain norm Eq. 4, the right-hand side of Eq. 3 becomes

$$\|\mathbf{FLC}\| = \text{FLC}_1 \cdot \eta(1,\beta) \ \ \text{with} \ \ \beta = \frac{\Delta \text{FLC}_2^*}{\Delta \text{FLC}_1^*} \tag{11}$$

Inserting this expression in Eq. 3 yields the final strain solutions

$$\text{FLC}_1 = \frac{\|\boldsymbol{\varepsilon}^*\| + \|\mathbf{FLC}^* - \boldsymbol{\varepsilon}^*\|}{\eta(1,\beta)}, \ \ \text{FLC}_2 = \beta \cdot \text{FLC}_1 \tag{12}$$

Most importantly, the *inverse retro analysis* enables the *removal of pre-strain effects* from a given FLC, which is very attractive to the sheet metal forming community, because it allows to correct experimental data accordingly, see below.

Remark. It should be mentioned that a similar strain-path correction approach was developed by Leppin et al. [6], who incrementally followed the nonlinear strain-paths recorded during their Nakajima tests. Basically, their incremental procedure is the most consistent approach, but it has some important disadvantages: (i) it presumes a measurement system equipped with the necessary data acquisition, which is not available in all laboratories; (ii) the strain measurement errors accumulate; (iii) for the sake of consistency, the bending strain compensation must be *incrementally* employed, and any approximations associated with the underlying bending correction theory accumulate. Obviously, the latter contributions will bias the integrated strains to some extent. As a final remark, the approach of Leppin et al. [6] accounts *implicitly* for pre-strains, whereas the approach developed in the present work takes pre-strains *explicitly* into account, thereby enabling both a forward and an inverse retro analysis.

Bending Strain Analysis
Introduction. The overall objective is to calculate the *midplane* strains of the deformed Nakajima sample from known (measured) surface strains. For this purpose, the strain theory for shell bending derived in Timoshenko & Gere [10] is employed.
General equations. According to Timoshenko & Gere [10, pp. 440-441], the surface strains of a bent shell can be calculated from

$$e_j(z) = \frac{e_{j,\text{mid}}}{1 - z/R_j} - \frac{z}{1 - z/R_j} \cdot \left[\frac{1}{(1 - e_{j,\text{mid}}) \cdot \hat{R}_j} - \frac{1}{R_j} \right], \ \ j = 1,2 \tag{13}$$

with R_j and $\hat{R}_j$ denoting the radius of curvature in the undeformed and deformed configuration, respectively. The coordinate z points towards the center point of curvature and is zero in the shell's midplane. Accordingly, at the convex side of the shell $z = -t/2$ and at the concave side $z = +t/2$, with t being the shell's thickness. The respective strain in the midplane is $e_{j,\mathrm{mid}}$. Note that all strains in Eq. 13 are *engineering* strains. In the *undeformed* configuration the blank is *flat*, i.e. $R_j \to \infty$. Accordingly, Eq. 13 simplifies to

$$e_j(z) = e_{j,\mathrm{mid}} - \frac{z}{(1-e_{j,\mathrm{mid}})\cdot\hat{R}_j}, \quad j = 1,2 \tag{14}$$

We consider the strains at the *convex* surface of the deformed sample, i.e. at $z = -t/2$, which are assumed of being known from measurements:

$$e_{j,\mathrm{surf}} := e_j(z = -t/2) = e_{j,\mathrm{mid}} + \frac{t/2}{(1-e_{j,\mathrm{mid}})\cdot\hat{R}_j}, \quad j = 1,2 \tag{15}$$

This may be rearranged to give the following quadratic equation in terms of $e_{j,\mathrm{mid}}$:

$$\left(e_{j,\mathrm{mid}}\right)^2 + \left(-1 - e_{j,\mathrm{surf}}\right)\cdot e_{j,\mathrm{mid}} + \left(e_{j,\mathrm{surf}} - \frac{t/2}{\hat{R}_j}\right) = 0, \quad j = 1,2 \tag{16}$$

This equation possesses two possible solutions, but only the following one yields physically plausible results:

$$e_{j,\mathrm{mid}} = \frac{1+e_{j,\mathrm{surf}}}{2} - \sqrt{\left(\frac{1+e_{j,\mathrm{surf}}}{2}\right)^2 - \left(e_{j,\mathrm{surf}} - \frac{t/2}{\hat{R}_j}\right)}, \quad j = 1,2 \tag{17}$$

The *engineering* midplane strains can be converted to *logarithmic* strains, and vice versa, according to

$$\varepsilon_j = \ln(1 + e_j) \iff e_j = \exp(\varepsilon_j) - 1, \quad j = 1,2 \tag{18}$$

Application to the Nakajima test. The strain theory may be transferred to the Nakajima test as follows. Regarding the midplane's radius of curvature, we assume

$$\hat{R}_1 = \hat{R}_2 = R_\mathrm{p} + t/2 \tag{19}$$

with the punch radius R_p and the *current* sheet thickness t. The *engineering* midplane strains $e_{j,\mathrm{mid}}$ can be computed from the *measured* surface strains at failure (constituting the given Nakajima FLC) using Eq. 17 as follows:

$$e_{j,\mathrm{mid}} = \frac{1+e_{j,\mathrm{surf}}}{2} - \sqrt{\left(\frac{1+e_{j,\mathrm{surf}}}{2}\right)^2 - \left(e_{j,\mathrm{surf}} - \frac{t/2}{R_\mathrm{p}+t/2}\right)}, \quad j = 1,2 \tag{20}$$

Before entering Eq. 20, the logarithmic surface strains must be converted to engineering strains using Eq. 18, and after evaluation of Eq. 20 the engineering strains $e_{j,\mathrm{mid}}$ can be converted back to logarithmic strains.

Using concise notation, we may summarize the outlined computation as follows:

1. Input: punch radius R_p; initial blank thickness t_0; measured surface strains $\varepsilon_{j,\mathrm{surf}}$, $j = 1,2$
2. Calculate current blank thickness: $t = t_0 \cdot \exp\left(-(\varepsilon_{1,\mathrm{surf}} + \varepsilon_{2,\mathrm{surf}})\right)$
3. Convert to engineering strains: $e_{j,\mathrm{surf}} = \exp(\varepsilon_{j,\mathrm{surf}}) - 1, j = 1,2$
4. Calculate midplane strains: $e_{j,\mathrm{mid}} = \mathrm{surface2midplane}(e_{j,\mathrm{surf}}, R_\mathrm{p}, t)$, $j = 1,2$
5. Convert to logarithmic strains (output): $\varepsilon_{j,\mathrm{mid}} = \ln(1 + e_{j,\mathrm{mid}}), j = 1,2$

The logarithmic midplane strains are regarded as to constitute a bending compensated FLC. In general, the bending strains must be subtracted from the FLC data *before* the pre-strains are removed.

Remark. Hill [5, p. 287] rates

$$\text{neutral plane} \approx \text{central plane throughout bending} \tag{21}$$

as a good approximation for plane-strain bending, provided that the radius of curvature is larger than four to five times the sheet's thickness. Furthermore, in a detailed analysis, assuming *ideal-plastic* material behavior, Hill [5, p. 293] and Lippmann [7, p. 94] derived the radius of the neutral surface in plane-strain *bending under tension* of sheets as $\hat{R} = \sqrt{R_\mathrm{i} \cdot R_\mathrm{o}} \cdot \exp\left(-p/(4k)\right)$, with R_i and R_o being the inner and outer radius of the bent sheet, respectively, p the contact pressure caused by the bending tool and k the material's shear yield stress. Even this result suggests that the approximation in Eq. 21 can be justified under usual conditions if p is not too large compared to the yield stress.

Application Example I
The intention of the considered application example is to demonstrate the capabilities of the *forward retro analysis*. In the following scenario we consider two user-supplied reference FLCs, which are assumed of being given:

1. A user-supplied FLC based on linear strain-paths, called FLC.
2. A user-supplied FLC based on bi-linear strain-paths, called FLC*.

Both FLCs were calculated using the elastic-plastic CST/M-K necking model, as described in detail in the paper of Aretz [2], because in a simulation model the pre-strains can be prescribed *exactly*, which is impossible in experiments. Bending strains are *absent* in all FLC simulations.

The material considered in all FLC simulations is a rolled sheet made of the aluminium alloy AA2008-T4, whose material data were taken from the paper of Lege et al. [4]. In accordance with the said reference, the yield surface was described by means of the orthotropic non-quadratic "Yld89" yield function (cf. Barlat & Lian [3]), whose material dependent parameters are $a = 0.119316\mathrm{E}+01$, $h = 0.115889\mathrm{E}+01$, $p = 0.102435\mathrm{E}+01$, along with the yield function's exponent $M = 8$. Isotropic hardening was assumed, and the hardening curve was described using the Voce ansatz function of the form $Y_\mathrm{ref}(\bar{\varepsilon}) = A - B \cdot \exp\left(-C \cdot \bar{\varepsilon}\right)$ with the parameters $A = 408$, $B = 233$ and $C = 6.14$.

Table 1. Definition of the considered pre-straining scenarios.

Scenario No.	Pre-strains $\{\varepsilon_2^*, \varepsilon_1^*\}$
1	$\{-0.04, 0.1\}$
2	$\{0, 0.1\}$
3	$\{0.05, 0.05\}$

In all FLC simulations the *same* material model was used, and only the pre-straining according to Table 1 was varied. The FLC simulation results pertaining to zero and non-zero pre-strains are shown in Fig. 1, labelled as "FLC (sim.)" and "FLC* (sim.)", respectively. The objective is to use

the forward retro analysis to calculate FLC* from FLC for the pre-straining scenarios defined in Table 1. The results of these analyses are labelled as "FLC* (forward retro)" in Fig. 1, and reveal that $\mathbf{FLC}^* \approx \mathrm{retro}(\mathbf{FLC}, \boldsymbol{\varepsilon}^*)$ holds with very good accuracy (compare grey and green curves) in each scenario.
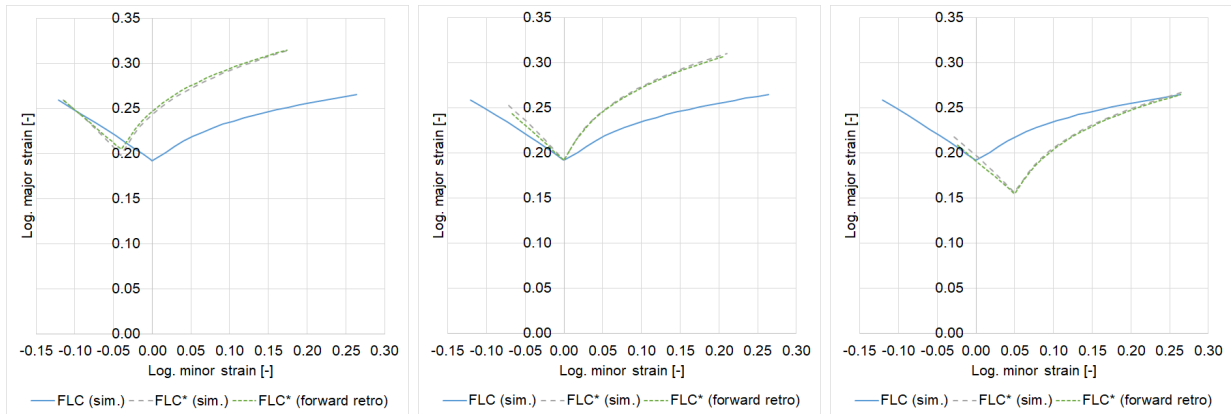

Figure 1. Forward retro analysis results for different pre-straining scenarios (cf. Table 1); from left to right: $\{\varepsilon_2^*, \varepsilon_1^*\} = \{-0.04, 0.1\}$, $\{\varepsilon_2^*, \varepsilon_1^*\} = \{0, 0.1\}$ and $\{\varepsilon_2^*, \varepsilon_1^*\} = \{0.05, 0.05\}$.

Application Example II

The intention of the second application example is to demonstrate the capabilities of the *inverse retro analysis*. Here, the pre-straining scenario no. 1 defined in Table 1 is considered. Figure 2 summarizes the associated results.

The reference FLC shown in Fig. 2 (left), labelled as "Reference (input)", pertains to zero pre-strains and is identical to the previous application example. Application of the forward retro analysis to the FLC "Reference (input)", along with the pre-strains $\{\varepsilon_2^*, \varepsilon_1^*\} = \{-0.04, 0.1\}$, yields the FLC "Forward retro (output)" in Fig. 2 (left).

In Fig. 2 (right) the process is reversed: the results of the previous forward retro analysis, now labelled as "Forward retro (input)" in Fig. 2 (right), are fed to the inverse retro analysis, yielding the FLC "Inverse retro (output)" in Fig. 2 (right), which is *identical* to the FLC "Reference (input)" in Fig. 2 (left). This confirms the important theoretical prerequisite

$$\mathbf{FLC} = \mathrm{retro}^{-1}(\mathrm{retro}(\mathbf{FLC}, \boldsymbol{\varepsilon}^*), \boldsymbol{\varepsilon}^*) \tag{22}$$

which means that the forward and inverse retro analysis neutralize each other.
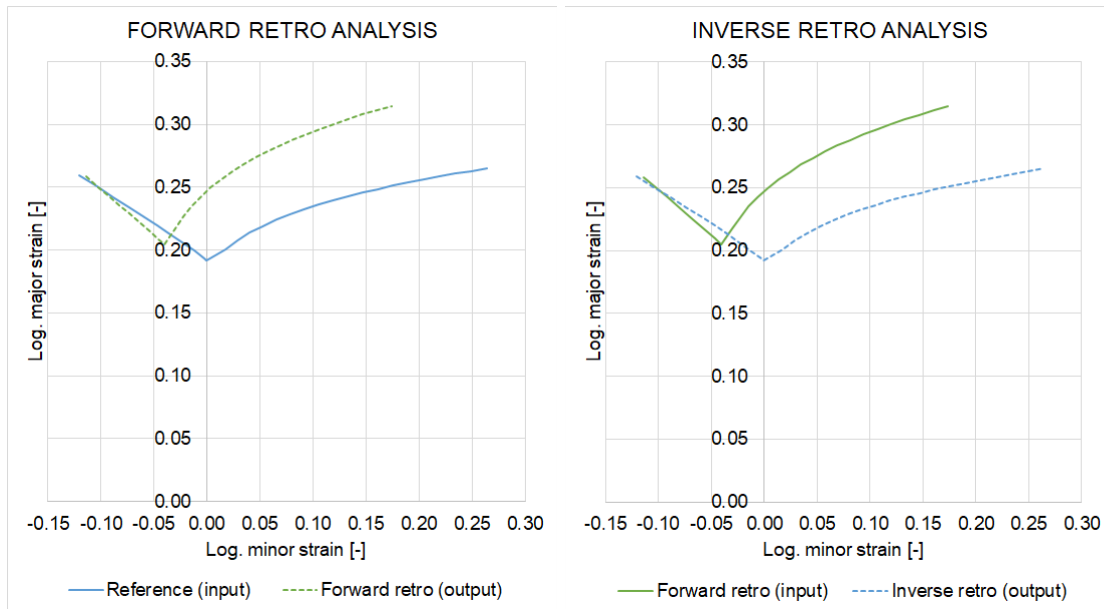
Figure 2. Inverse retro analysis results for the pre-straining scenario no. 1 (cf. Table 1).

Application Example III

In the last application example, measured FLCs acquired by Nakajima tests are considered, which are intrinsically biased by pre-strains. Therefore, these FLCs will be labelled as FLC^*. Both pre-strains and bending strains will be removed from the FLC^* data as described above. In what follows, it is assumed that pre-straining occurred under *equibiaxial tension*, and that the minor strain value of the pre-strains equals the minor strain of FLC^*_{min}, which reads in concise notation $\varepsilon_1^* = \varepsilon_2^* = (\mathbf{FLC}^*_{min})_2$. The punch radius used in the Nakajima experiments was $R_p = 50$ mm, which is required for the bending strain calculation. It is important that the bending strain correction is carried out *before* the pre-strain correction.

The considered materials were made of two aluminium alloys of the 5000 class with different gauges (1.5 mm and 2.5 mm, respectively), which leads to different contributions of the respective bending correction. For both materials FLCs were determined according to the DIN EN ISO 12004-2 standard, with 3 repetitions for each sample geometry. The averaged results are shown in Fig. 3 (labelled as "Input"). In the first step, the bending strains were corrected, i.e. the midplane strains were calculated from the measured surface strains, yielding the intermediate results labelled as "Bending correction" in Fig. 3. Thereafter, these midplane strains are fed to the inverse retro analysis, along with the pre-strains $\varepsilon_1^* = \varepsilon_2^* = (\mathbf{FLC}^*_{min})_2$, yielding the final results labelled as "Output" in Fig. 3. It is very interesting to observe how the FLCs changed after the final correction step: while the FLC_{min}-point of the 1.5 mm material was significantly lifted in major strain direction, this is not the case for the 2.5 mm material, where the FLC_{min}-point experiences almost no change in terms of its major strain. The primary reason for this observation is that the thinner material's FLC^*_{min}-point is originally much more displaced along the minor strain axis, which causes a correspondingly large correction by the inverse retro analysis towards a larger major strain value. Furthermore, the bending correction is larger for the thicker material, i.e. the thicker material "looses" more major strain after bending correction than the thinner material, as substantiated below. As expected, after the final correction step FLC_{min} coincides with plane strain deformation in both cases, i.e. FLC_{min} has moved to the major strain axis.
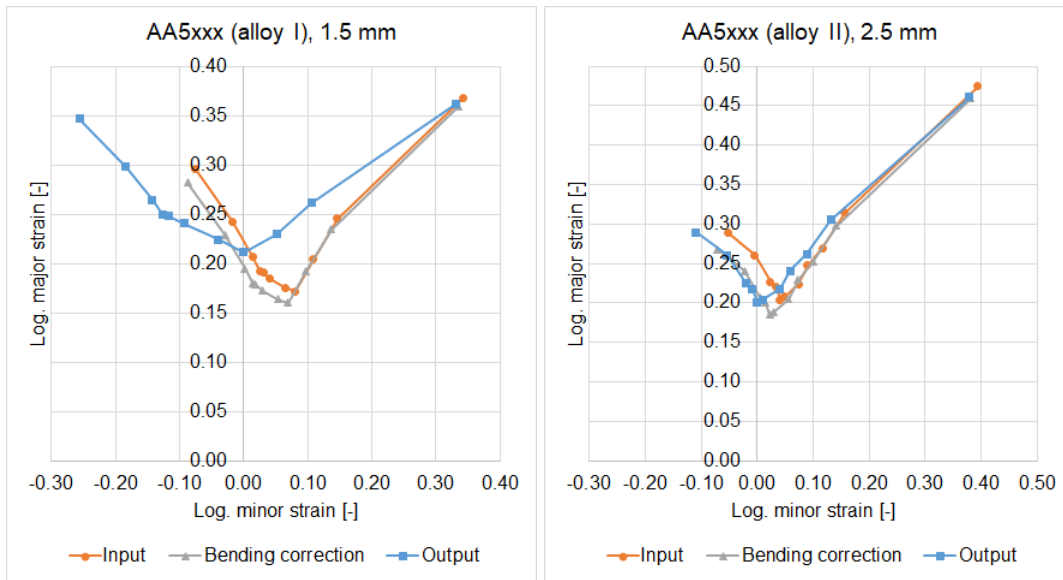
Figure 3. Bending correction followed by pre-strain correction using the inverse retro analysis for two materials made of 5xxx aluminium alloys with different compositions and gauges.
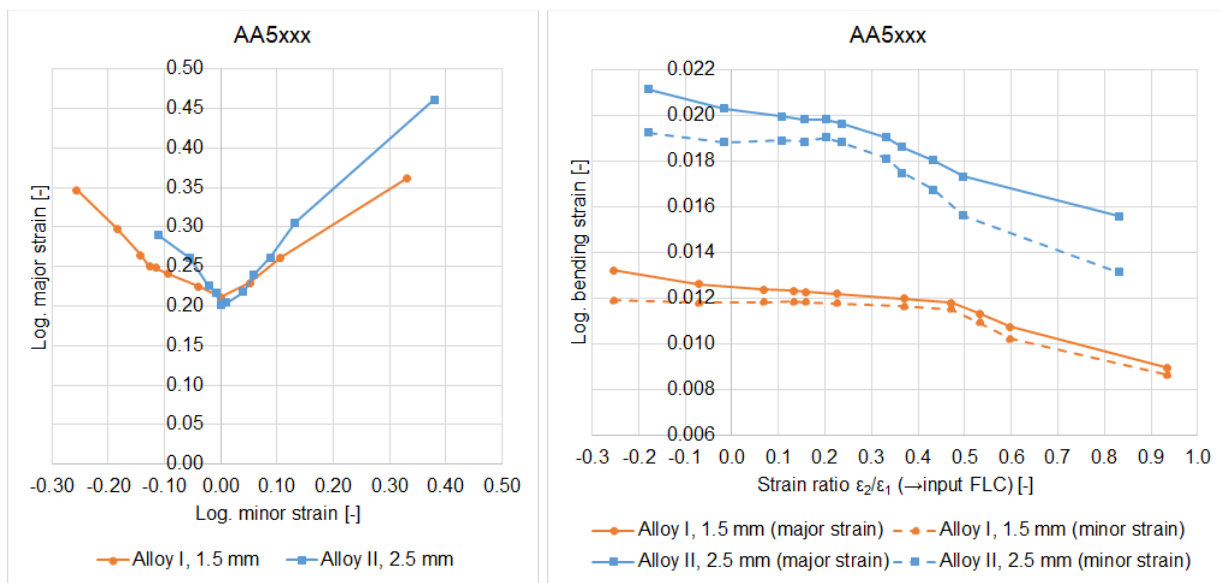

Figure 4. Direct comparison of the corrected FLC data shown in Fig. 3 (left) and calculated bending strains (right).

In Fig. 4 a direct comparison of both FLCs after the final correction step is shown. In accordance with the main motivation for the present work, it is now possible to compare different materials made of different gauges in terms of their respective FLC. In addition, Fig. 4 does also show the bending contribution in terms of the major and minor strains, calculated as the respective difference between the uncorrected FLC data and the corresponding data after bending correction, in accordance with Affronti & Merklein [1]. As expected, the bending strains are much larger in the case of the thicker material. Furthermore, one may see that the bending strain depends almost linearly on the strain ratio $\varepsilon_2/\varepsilon_1$: according to the results in Fig. 4, the smallest bending strain occurs in equibiaxial stretching and the largest one in the narrowest samples.

Summary

In the present work, a method to comprehensively correct FLC data acquired by means of the Nakajima test in terms of bending strains and pre-strains is proposed, which enables a direct comparison of FLCs pertaining to different materials made of different gauges.

It was demonstrated that the pre-strain correction reproduces theoretical results very well, and that it is self-consistent in the sense that it possesses the ability to neutralize itself, which is an important theoretical prerequisite.

The application of both the pre-strain and the bending correction to experimental data yields plausible results, but there are aspects of the proposed correction method which should be addressed in more detail in future work:

1. Regarding pre-strain correction, the following assumptions were implied: (i) the pre-strains can be identified as $\varepsilon_1^* = \varepsilon_2^* = (\mathbf{FLC}_{\min}^*)_2$ and (ii) these pre-strains can be *universally* assigned to *all* FLC samples. The question is whether this rather simple approach is sufficiently accurate or needs to be refined.
2. The proposed bending strain correction is based on the shell bending kinematics found in the textbook of Timoshenko & Gere [10, pp. 440-441]. The associated assumptions introduced in the present work (e.g. Eq. 19) should be carefully verified and, if necessary, revised in future work.

Acknowledgements

References

[1] E. Affronti, M. Merklein: Analysis of the bending effects and the biaxial pre-straining in sheet metal stretch forming processes for the determination of the forming limits, Int. J. of Mechanical Sciences 138-139 (2018) 295-309. https://doi.org/10.1016/j.ijmecsci.2018.02.024

[2] H. Aretz: An extension of Hill's localized necking model, Int. J. of Engineering Science 48 (2010) 312-331. https://doi.org/10.1016/j.ijengsci.2009.09.007

[3] F. Barlat, J. Lian: Plastic behaviour and stretchability of sheet metals – Part I: A yield function for orthotropic sheets under plane stress condition, Int. J. of Plasticity 5 (1989) 51-66. https://doi.org/10.1016/0749-6419(89)90019-3

[4] D. J. Lege, F. Barlat, J. C. Brem: Characterization and modeling of the mechanical behavior and formability of a 2008-T4 sheet sample, Int. J. of Mechanical Sciences 31 (1989) 549-563. https://doi.org/10.1016/0020-7403(89)90104-5

[5] R. Hill: *The Mathematical Theory of Plasticity*, Oxford University Press, 1950 (Reprinted 2009)

[6] C. Leppin, J. Li, D. Daniel: Application of a method to correct the effect of non-proportional strain paths on Nakajima test based forming limit curves, Proc. Numisheet 2008 Conference, Interlaken, Switzerland

[7] H. Lippmann: *Mechanik des plastischen Fließens*, Springer-Verlag, 1981. https://doi.org/10.1007/978-3-642-52209-3

[8] W. Müschenborn, H.-M. Sonne: Einfluß des Formänderungsweges auf die Grenzformänderungen des Feinblechs, Archiv des Eisenhüttenwesens 46 (1975) 597-602. https://doi.org/10.1002/srin.197503686

[9] J. Noder, C. Butcher: A comparative investigation into the influence of the constitutive model on the prediction of in-plane formability for Nakajima and Marciniak tests, Int. J. of Mechanical Sciences 163 (2019) 105138. https://doi.org/10.1016/j.ijmecsci.2019.105138

[10] S. Timoshenko. J. M. Gere: *Theory of Elastic Stability*, 2nd ed., Dover Publication, 2009